The Influence of the Electrophoretic and Polarization Forces on Two Phase Flow Redistribution in a Horizontal Annular Tube

S. Nangle-Smith, H. Sadek, and J. S. Cotton
Department of Mechanical Engineering, McMaster University, Canada

Abstract—The objective of this study is to investigate the effect of high voltage DC waveforms on two phase flow redistribution. The flow patterns in a two phase flow system directly influences the system heat transfer and pressure drop, and by extension, the system performance. Electrohydrodynamics (EHD) induces flow pattern redistribution and therefore can provide a low power, rapid method of enhancement of two phase flow systems such as heat exchangers. The heat transfer characteristics can be varied by modifying the proportion of liquid or vapor in contact with the heat transfer surface. This study investigates the effect of the electrophoretic and polarization components of the EHD force on two phase flow redistribution in an annular channel for comparable cases of condensation and evaporation.

Keywords—Electrohydrodynamics, two-phase flow, polarity, electrophoretic, polarization

I. Introduction

The EHD body force term in the fluid momentum equations causes flow redistribution. For dielectric two phase flows, the force is composed of three terms as shown in equation (1).

$$\overline{f_{eB}} = \rho_{ei}\overline{E} - \frac{1}{2}E^2\nabla\varepsilon + \frac{1}{2}\nabla\rho E^2\left(\frac{\partial\varepsilon}{\partial\rho}\right)_T \quad (1)$$

The first term is known as the electrophoretic or Coulomb force. This force acts on free ions or charges within the fluid and causes them to migrate along electric field lines, a phenomenon known as electroconvection [1]. The electrophoretic force is dominant in single phase applications, where there is little change in the permittivity, ε, of the fluid. In two phase applications there will be electroconvection currents in both the liquid and vapor phases due to this force. This force component is proportional to the electric field, E, unlike the other two forces which are proportional to E^2. Therefore the effect of polarity manifests in this force. The electrophoretic force is proportional to the volume charge density, ρ_{ei}, in the fluid and so charge injection plays a role. For refrigerant systems similar to our design, Ng [2] suggested that the mechanism of charge injection is always negative charges from the negative electrode based on the mobility model proposed by Fujino *et al*. [3]. The second and third terms of equation (1) are known collectively as the polarization forces. They polarize or stretch the molecules in the dielectric. The dielectrophoretic force arises due to the spatial change in permittivity. The permittivity can be spatially inhomogeneous due to non-uniform electric fields, changes in phase, temperature, T, and density, ρ, gradients in the flow. The electrostrictive term arises due to the change in permittivity with density which can be due to local concentrations (i.e. fluid additives, suspended droplets, boundary layers etc.) or temperature gradients in the flow. Large gradients in permittivity exist at the liquid-vapor interface for two phase systems. The polarization forces as a result of this interfacial stress are larger than the electrophoretic force by an order of magnitude [4]. Phase redistribution occurs due to the difference in relative permittivity between the phases; 9.5 for the R134a liquid and approximately 1 for the R134a vapor. The liquid phase is attracted to regions of high electric field due to its higher permittivity, a phenomenon known as liquid extraction [1]. Fig. 1 summarizes the effect of EHD forces on various components in a flow system.

The main influences on flow pattern in a system are the system geometry (including objects that disturb the flow), orientation (gravitational effects), temperature dependent fluid properties, surface tension in particular, the flow rates and the proportion of liquid and vapor in

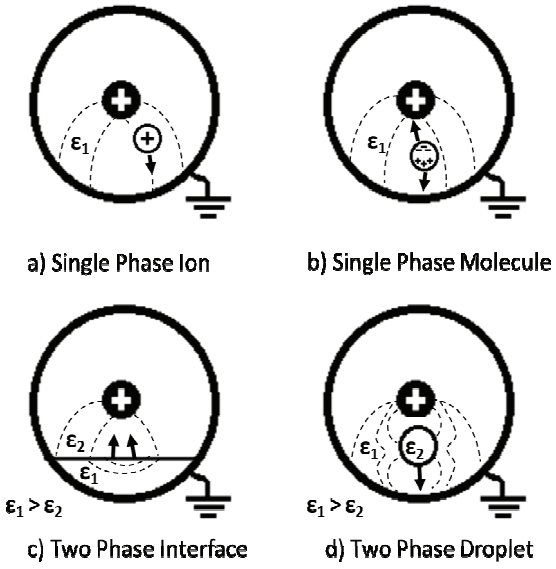

Fig. 1. Effect of EHD on flow redistribution.

Corresponding author: James S. Cotton
e-mail address: cottonjs@mcmaster.ca

Presented at the 2012 International Symposium on Electrohydrodynamics (ISEHD 2012), in September 2012

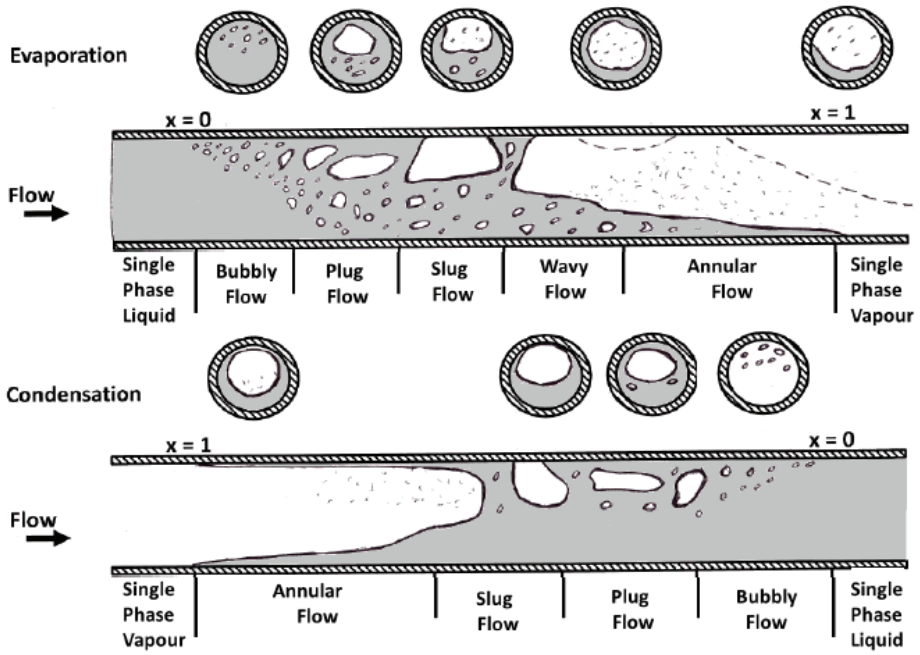

Fig. 2. Convective boiling (top) & convective condensation (bottom) horizontal flow patterns (adapted from Collier [15])

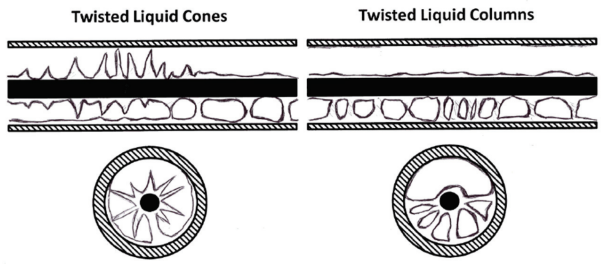

Fig. 3. EHD flow patterns

the system, i.e. the flow quality, *x*. The flow patterns for convective boiling and convective condensation in a horizontal tube are shown schematically in Fig. 2. The main difference between the two is that an annular flow regime exists at higher vapor qualities in condensation than for evaporation. EHD can induce new flow patterns, e.g. twisted liquid cones and columns, as shown in Fig. 3 [2, 5].

Flow pattern maps have been developed as a predictive design tool. Theoretically based maps are recommended as they are applicable to all types of flow systems, e.g. the Taitel and Dukler general flow pattern map [6], the El Hajal *et al.* map for convective condensation [7] and Kattan's map [8] for convective boiling. The Steiner map [9] incorporates the effect of an annular geometry on flow patterns. Cotton [4] developed an EHD flow pattern map which incorporates the EHD induced interfacial force into the Steiner analytical model to predict the transition from stratified to annular flow. It was found that when using EHD this transition can occur at lower flow rates.

Most convective boiling studies use long test sections, 1-3 m in length [1, 4, 10]. Although these lengths are typically those found for evaporators in industry, it is impossible to maintain a constant flow pattern when the quality varies so greatly across the length. Since EHD is known to change the flow pattern distribution and experimental parameters which quantify the effects of EHD, e.g. heat transfer coefficient, are highly dependent on specific flow patterns, it is necessary to maintain a consistent flow pattern to gain insight into the true effects of EHD. Some researchers that have used short, 300mm, test sections for EHD convective boiling [12-14]. In this study, a short test section is used to maintain a consistent flow pattern along the tube and to determine the effect of DC high voltage on convective boiling and condensation flow redistribution.

II. Methodology

Convective boiling and condensation tests subject to electrohydrodynamics (EHD) were conducted in a horizontal, counter-current, shell and tube heat exchanger. The test rig used in this study is the same as that used in studies by Sadek and Ng [2, 16]. The test section is shown Fig. 4. The outer tube, inner diameter 10.2 mm, is grounded and voltage is applied via a concentric stainless steel electrode, outer diameter 3.2 mm. The test section is 300 mm long allowing for a consistent flow pattern along the tube length. DC voltages of varying polarity and amplitude up to ±8 kV were tested for the following flow conditions: Mass flux, G: 60 kg/m^{2}s, Average Quality, Xav: 40%, inlet and outlet quality difference, ΔX: 10%. The applied water side heat flux, q", was positive or

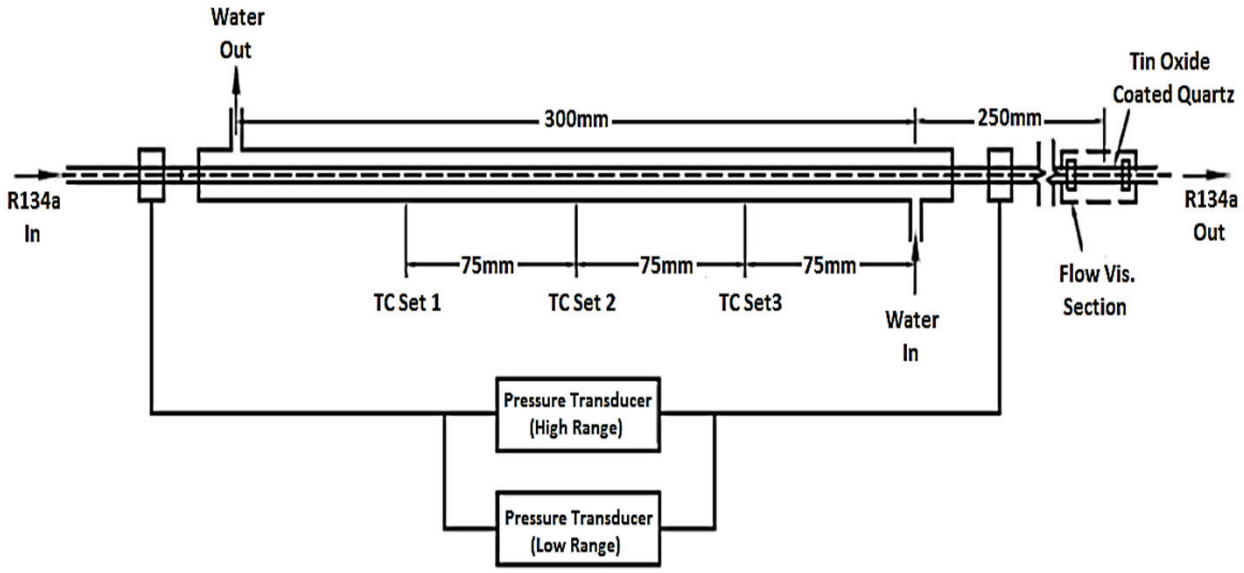

Fig. 4. Test section schematic.

TABLE I
EXPERIMENTAL UNCERTAINTIES

Measurement, x		Precision error	Bias error	Total
RTD ΔT_{water}	°C	±0.08	±0.04	±0.09
Thermocouple temp.	°C	±0.24	±0.22	±0.33
Refrigerant flow rate	kg/s	$\pm 1.2\times10^{-3}$	$\pm 1.3\times10^{-5}$	$\pm 1.2\times10^{-3}$
Water flow rate	kg/s	$\pm 2\times10^{-4}$	$\pm 3\times10^{-4}$	$\pm 3.6\times10^{-4}$
Pressure drop (Low)	Pa	±10	±11	±15
Pressure drop (High)	Pa	±18	±13	±23
Parameter, f			Relative uncertainty	
Heat flux, q"	kW/m^2		±12%	
Heat transfer coefficient, h	W/m^2K		±13%	
Inlet quality, X_{in}	dim		±23%	
System energy balance			within ±5%	

negative 8-9 kW/m^2 for condensation or evaporation respectively. Table I shows the experimental uncertainties and the overall system energy balance. The flow parameters were chosen to maintain a wavy liquid stratum below the electrode along the test section before the application of EHD to assess the mechanism of transition to other flow distributions, similar to the analysis of Taitel and Dukler [6]. It has been shown that this flow distribution allows for high interfacial EHD forces induced by the proximity of the two phase interface to the electrode for a shell and tube heat exchanger system [17].

The water side heat flux is calculated as:

$$q''_{water} = \dot{m}_{water} C_{P,water} \Delta T_{water} \quad (2)$$

Also, the average heat transfer coefficient is calculated as

$$h_{av} = \frac{q''_{water}}{A_s \left(T_{ref,sat} - T_{s,av} \right)} \quad (3)$$

where $\dot{m}$ is the flow rate, C_p is the specific heat capacity of the water, ΔT_{water} is the water temperature difference measured using a RTD, As is the heat exchanger surface area, $T_{ref,sat}$ is the saturated refrigerant temperature and $T_{s,avg}$ is the average surface temperature.

III. RESULTS AND DISCUSSION

Fig. 5 shows the flow visualization using a Photron high speed camera and the associated estimated static electric field distribution for the onset of high voltage application in a stratified wavy flow system. The electric field distribution was calculated using Comsol maintaining a constant void fraction, $\alpha = 0.164$, between each case, i.e. the same cross sectional area of liquid.

The electric field ranges from 8×10^4 to 3.3×10^6 V/m, with the darker areas indicating areas with higher electric field. Fig. 5a suggests that the electric field is strongest at the bottom of the electrode and thus, the interfacial force is highest at the midpoint of the interface. This causes the liquid to be extracted toward the electrode. The interfacial force increases with decreasing electrode-liquid gap distance and with increasing electric field strength. If this force is high enough the liquid level will reach the electrode. From the flow visualization we can see that liquid extraction is occurring due to this electric field distribution.

The electric field distribution changes when the liquid level reaches the electrode. The region of highest electric field is now at the electrode, either side of the liquid region. Therefore the liquid tends to be pulled around the electrode surface due to the polarization forces at the interface and is possibly partially aided by surface tension effects. When the liquid has fully surrounded the electrode, as seen in Fig. 5d, the electric field is inverted, with the strongest region being at the liquid-vapor interface offset from the electrode. This will

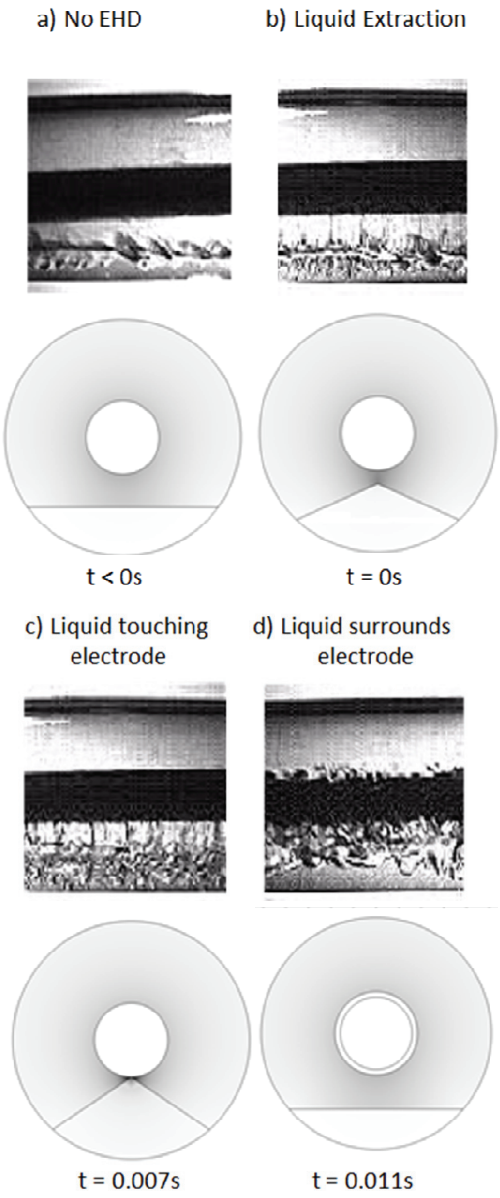

Fig. 5. DC voltage flow visualization and electric field analysis.

induce a polarization force that repels the liquid away from the electrode.

The mechanism of liquid repulsion is different for positive and negative applied voltages and results in different flow patterns as can be seen in the flow visualization in Fig. 6. Positive voltages give rise to twisted liquid conical structures and Negative voltages induce twisted liquid column-like structures below the electrode. These differing flow patterns based on polarity were also seen by Ng [16].

It is suggested here that the electrophoretic force contributes the most to the difference in repulsion between positive and negative applied voltage since it is the component where polarity has a dominant effect. In the case of negative applied voltage, the electrophoretic force aids the repulsion force whereas in the case of positive applied voltage, the electrophoretic force acts against the repulsion force. For the case of a negative

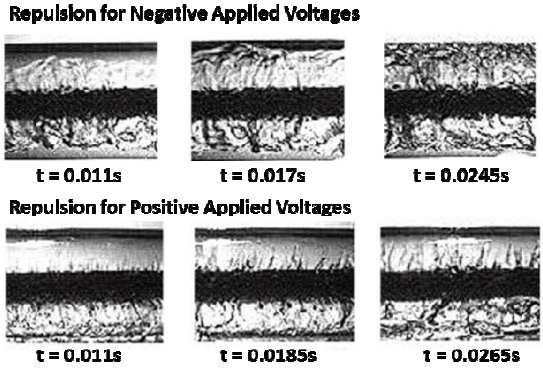

Fig. 6. DC voltage flow visualization - liquid repulsion.

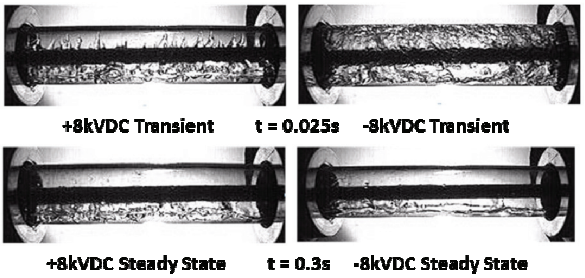

Fig. 7. Transient and steady state EHD patterns.

applied voltage, charge is injected from the negative electrode liquid annulus surrounding the electrode. The liquid annulus becomes negatively charged and this causes it to be repelled from the negative electrode. The wavy flow on the bottom electrode is not charged unless there is a gap bridged between this and the liquid surrounding the electrode. This liquid stratum is extracted toward the electrode and repelled upon reaching the electrode. For the case of a positive polarity, the liquid surrounding the electrode is positively charged and will be repelled from the positive electrode. However, charge injection of negative ions occurs from the outer tube into the wavy flow in contact with this surface underneath the electrode. This negatively charged liquid will be highly attracted toward the positive electrode both due to polarization and electrophoretic forces. When this liquid is extracted and surrounds the electrode it acts against the liquid being repelled from the positively charged electrode. This extraction and surrounding occurs continually and the proposed result is an inverted annular flow with some conical regions of liquid repulsion.

The transient flow patterns occurring milliseconds after the application of high voltage are shown in Figs. 5 and 6. After approximately 520 ms the electrophoretic and polarization forces balance out and a steady state will exist. [16]. Steady state flow patterns are less turbulent than the transient flow patterns but the differences in liquid repulsion mechanisms for opposing polarities still exist as seen in Fig. 7. The transient flow patterns provide insight into the phenomenon of EHD but the steady state data, taken after 10 minutes, is used for all heat transfer and pressure drop readings.

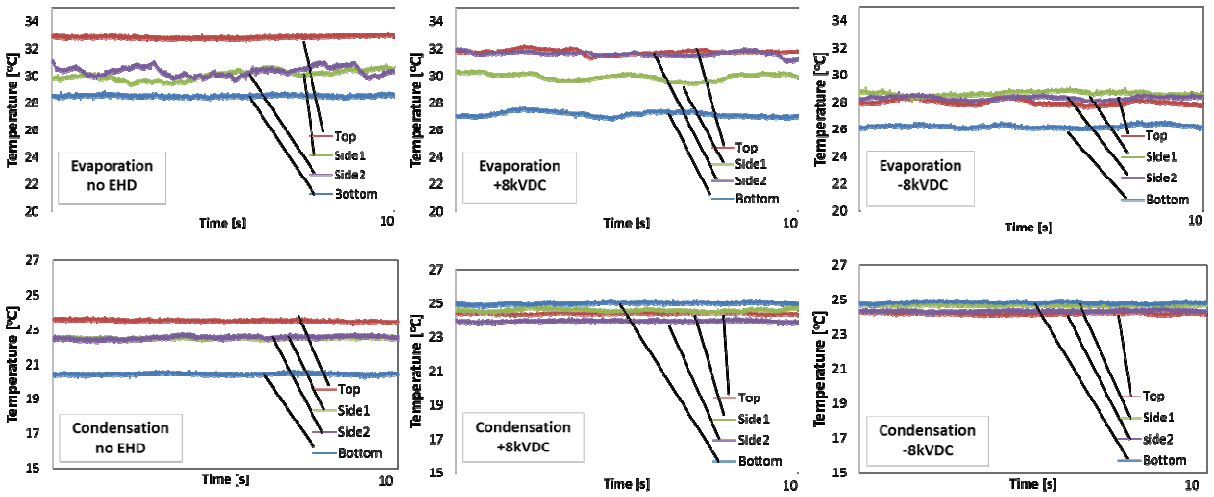

Fig. 8. Surface temperature profiles at axial location 2. evaporation (top), condensation (bottom).

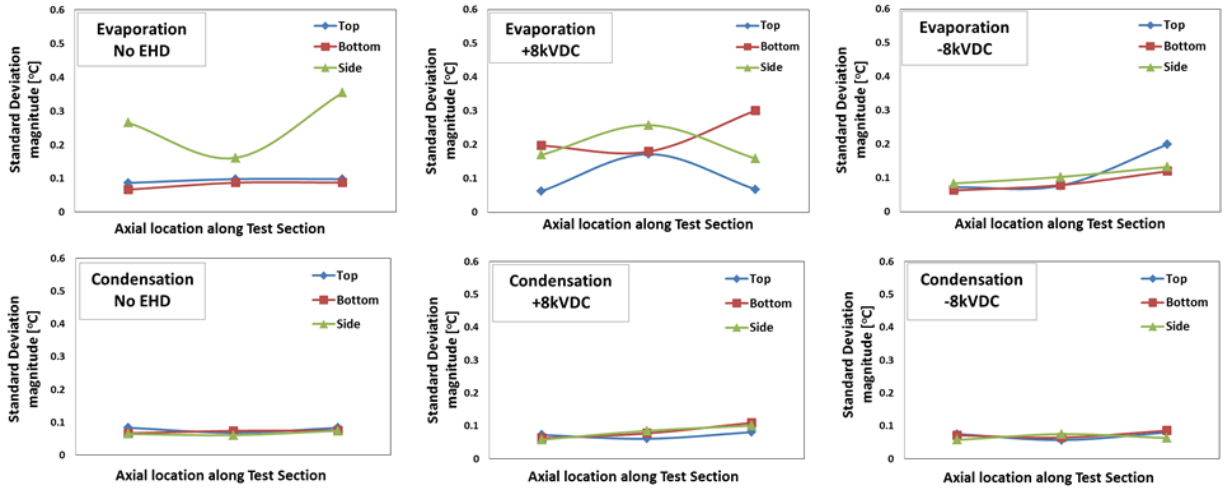

Fig. 9. Surface temperature associated standard deviations. evaporation (top), condensation (bottom).

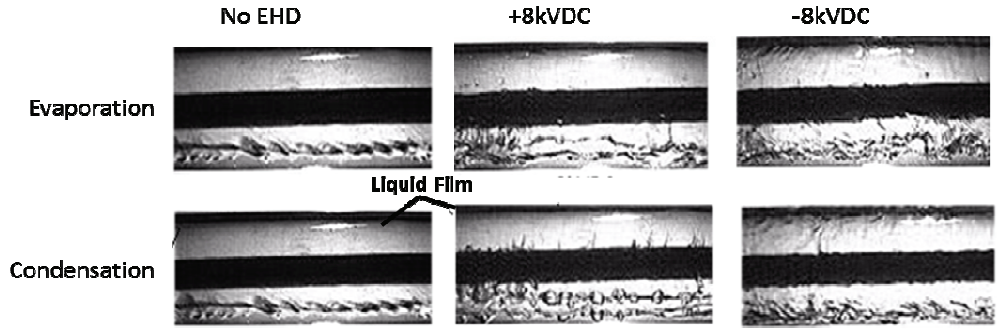

Fig. 10. Flow visualization. evaporation (top), condensation (bottom).

The flow redistribution due to EHD can be studied via flow visualization or by analysis of the surface temperature profiles and their associated standard deviations along the test section. The surface temperatures show are all for location 2 i.e. the middle of the test section. (See Fig. 4)

For the no EHD evaporation case, the bottom temperature is approximately 28°C, the top is approximately 33°C (Fig. 8) and the associated standard deviation (Fig. 9) is low, 0.06°C approximately. This suggests a stratified flow pattern with liquid at the bottom and vapor at the top. The side temperatures vary between 28°C and 33°C with high variance, 0.2°C approximately, suggesting a wavy interface that wets the side. The corresponding flow images in Fig. 10 confirm this flow pattern. The no EHD condensation case (Fig. 8)

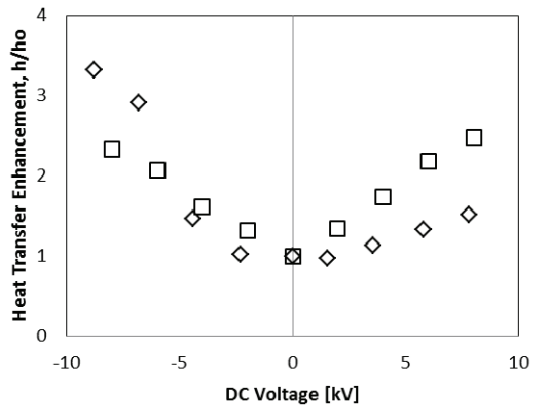

Fig. 11. Heat transfer enhancement comparison: The effect of DC applied voltage, G = 60 kg/m^{2}s, q" = ±8.5 kW/m^2, X_{av} = 40%. ◊ Evaporation, □ Condensation

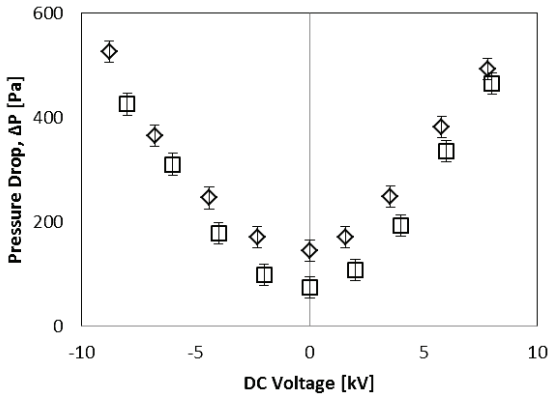

Fig. 12. Pressure drop comparison: The effect of DC applied voltage, G = 60 kg/m^{2}s, q" = ±8.5 kW/m^2, X_{av} = 40%. ◊ Evaporation, □ Condensation

is quite similar to its evaporation counterpart except the temperatures are lower, closer in value and all have a low standard deviation, 0.06^{o}C approximately. Thinner liquid films in condensation coincide with higher temperatures. This suggests that liquid film is present at all of the measurement locations in addition to the stratified flow pattern and this is confirmed in Fig. 10.

For the case of positive 8 kVDC, Figs. 8 and 9 show intermittent top and side temperatures in evaporation. This suggests an intermittent flow with varying liquid thicknesses. The flow visualization in Fig. 10 shows conical structures below the electrode, high turbulence, liquid in core region and some liquid droplets repelled from the electrode impinging on the heat transfer surface. A similar flow pattern is seen in Fig. 10 for the condensation case. The variance is low which may be due to the condensing liquid film present on the top and sides surfaces.

Finally for the case of negative 8 kVDC, Figs. 8 and 9 show similar top and side temperatures with low variance suggesting that there is liquid at these locations. Fig. 10 confirms an annular flow pattern has been established due to the liquid repulsion. The same flow pattern is suggested from Figs. 8 and 10 for the case of condensation. It seems that the stronger the electric field, the more similar the flow patterns become for condensation and evaporation. This makes sense as the effect of EHD becomes more dominant.

The heat transfer coefficient and the test section pressure drop are used to quantify the enhancement achieved with EHD. (Figs. 11 and 12 respectively) Higher voltages result in more flow redistribution and therefore higher enhancement and a higher pressure drop. For condensation there is approximately a 2.5 fold increase in heat transfer for positive applied voltage and approximately 2.4 fold increase for the negative applied voltage. The enhancement is approximately 1.5 fold for positive voltage and 4 fold for negative voltage for evaporation. See Fig. 11. The pressure drop penalty increases by approximately 4fold in both cases for the highest tested applied voltage. See Fig. 12.

The effect of polarity is apparent in this graph indicating that negative voltages are more suitable for convective boiling heat transfer enhancement and positive voltages more suitable for convective condensation heat transfer. It is hypothesized that heat transfer and pressure drop are primarily a function of flow pattern and that some flow patterns may be more favorable for different heat transfer mechanisms. Here, the positive applied voltage attracts more liquid into the core region drying the heat transfer surface. This is advantageous in condensation, where the vapor needs to be in contact with heat transfer surface to condense, but less efficient in boiling as portions of the heat transfer surface may be dry. The opposite is true for the case of negative applied voltage. Here more liquid is repelled toward the heat transfer surface. This is suitable for boiling as it rewets the heat transfer surface, but not as useful in condensation as it interferes with the ease of formation of condensing droplets.

IV. Conclusion

A short, 300 mm, test section was used to study the effect of EHD forces on flow redistribution in a horizontal, shell and tube heat exchanger subject to both boiling and condensation. The use of the short test section allows for a consistent flow pattern across the test section length which provides further insight into the true effect of EHD. Flow visualization and surface temperature measurements were used to study the two phase flow pattern redistribution under applied DC voltage.

It was found that polarity influences the flow distribution. For both polarities, the liquid is extracted toward the electrode due to the polarization forces acting at the liquid vapor interface. The flow then surrounds the electrode via liquid extraction as the liquid, which has a high dielectric constant, is attracted to the region of high electric field. Once the fluid surrounds the electrode, the liquid will be repelled due to the polarization forces arising from the now inverted electric field distribution. The electrophoretic force aids this repulsion for negative

voltages and opposes this force for positive voltages, generating new flow distributions which were seen via flow visualization and surface temperature profiles.

A liquid film on the heat transfer surface improves boiling heat transfer and removal of this film improves condensation heat transfer. Using this knowledge we were able to show that these flow distributions could be used to enhance different modes of heat transfer.

ACKNOWLEDGMENT

This work is partially sponsored by NSERC. The author would also like to thank Dr. Cotton, Dr. Ching, Dr. Sadek and Mr. Ng for their invaluable help throughout the project.

REFERENCES

[1] A. Yabe, T. Taketani, H. Maki, K. Takahashi, and Y. Nakadai, "Experimental study of electrohydrodynamically (EHD) enhanced evaporator for nonazeotropic mixtures," *ASHRAE Transactions*, vol. 98, pp. 455-460, 1992.

[2] K. Ng, "Mechanisms of electrohydrodynamic two-phase flow structures and the influence on heat transfer and pressure drop," M. Sc. Thesis, McMaster University, Hamilton, Canada, 2010.

[3] T. Fujino, Y. Yokoyama, and Y. H. Mori, "Augmentation of laminar forced-convective heat transfer by the application of a transverse electric field," *Journal of Heat Transfer,* vol. 111, pp. 345-351, 1989.

[4] J. Cotton, A. J. Robinson, M. Shoukri, and J. S. Chang, "A two-phase flow pattern map for annular channels under a DC applied voltage and the application to electrohydrodynamic convective boiling analysis," *International Journal of Heat and Mass Transfer,* vol. 48, pp. 5563-5579, 2005.

[5] H. Sadek, J. S. Cotton, C. Y. Ching, and M. Shoukri, "Effect of frequency on two-phase flow regimes under high-voltage AC electric fields," *Journal of Electrostatics,* vol. 66, pp. 25-31, 2008.

[6] Y. Taitel and A. E. Dukler, "A model for predicting flow regime transitions in horizontal and near horizontal gas-liquid flow," *AIChE Journal,* vol. 22, pp. 47-55, 1976.

[7] (a) J. El Hajal, J. R. Thome, and A. Cavallini, "Condensation in horizontal tubes, part 1: two-phase flow pattern map," *International Journal of Heat and Mass Transfer,* vol. 46, pp. 3349-3363, 2003. (b) J. R. Thome, J. El Hajal, and A. Cavallini, "Condensation in horizontal tubes, part 2: new heat transfer model based on flow regimes," *International Journal of Heat and Mass Transfer,* vol. 46, pp. 3365-3387, 2003.

[8] (a) N. Kattan, J. R. Thome, and D. Favrat, "Flow boiling in horizontal tubes: Part 1 - Development of a diabatic two-phase flow pattern map," *Journal of Heat Transfer-Transactions of the Asme,* vol. 120, pp. 140-147, 1998. (b) N. Kattan, J. R. Thome, and D. Favrat, "Flow boiling in horizontal tubes: Part 3 - Development of a new heat transfer model based on flow pattern," *Journal of Heat Transfer-Transactions of the Asme,* vol. 120, pp. 156-165, 1998.

[9] D. Steiner, *Heat Transfer to Boiling Saturated Liquids*, *VDI-Warmeatlas,*Verein Deutscher Ingenieure, ed. VDI-Gessellschaft Verfahrenstechnik und Chemieingenieurwesen (GCV), Dusseldorf, Germany, (Translator: J.W. Fullarton), 1993.

[10] A. Singh, M. M. Ohadi, S. Dessiatoun, and M. Salehi, "In-tube boiling enhancement of R134a utilizing the electric field effect," *ASME-JSME Papers*, vol. 2, pp. 215-223. 1995.

[11] J. S. Cotton, "Mechanisms of Electrohydrodynamic flow and heat transfer in horizontal convective boiling channels," Ph.D. Thesis, McMaster University, Hamilton, Canada, 2000.

[12] M. Salehi, M. M. Ohadi, and S. Dessiatoun, "Applicability of the EHD technique for convective boiling of refrigerant blends - experiments with R-404A," *ASHRAE Transactions,* vol. 102, pp. 839-844, 1996.

[13] M. Salehi, M. M. Ohadi, and S. Dessiatoun, "EHD enhanced convective boiling of R-134a in grooved channels - Application to subcompact heat exchangers," *Journal of Heat Transfer-Transactions of the Asme,* vol. 119, pp. 805-809, 1997.

[14] J. E. Bryan and J. Seyed-Yagoobi, "Influence of flow regime, heat flux, and mass flux on electrohydrodynamically enhanced convective boiling," *Journal of Heat Transfer-Transactions of the Asme,* vol. 123, pp. 355-367, 2001.

[15] J. G. Collier, *Convective Boiling and Condensation*, 2nd. s.l. : McGraw-Hill, New York, 1973.

[16] K. Ng, C. Y. Ching, and J. S. Cotton, "Transient Two-Phase Flow Patterns by Application of a High Voltage Pulse Width Modulated Signal and the Effect on Condensation Heat Transfer," *Journal of Heat Transfer-Transactions of the Asme,* vol. 133, 091501, 2011.

[17] H. Sadek, "Electrohydrodynamic control of convective condensation heat transfer and pressure drop in a horizontal annular channel," Ph.D. Thesis, McMaster University, Hamilton, Canada, 2009.